IEEE Access
Multidisciplinary ⋮ Rapid Review ⋮ Open Access Journal

Received 23 December 2023, accepted 9 January 2024, date of publication 16 January 2024, date of current version 30 January 2024.

Digital Object Identifier 10.1109/ACCESS.2024.3354891

RESEARCH ARTICLE

Decentralized Privacy-Preserving Distributionally Robust Restoration of Electricity/Natural-Gas Systems Considering Coordination of Pump Storage Hydropower and Wind Farms

N. NASIRI[1], (Student Member, IEEE), S. ZEYNALI[2], (Student Member, IEEE), S. NAJAFI RAVADANEGH[1], (Senior Member, IEEE), S. KUBLER[2], (Senior Member, IEEE), AND Y. LE TRAON[2], (Fellow, IEEE)

[1]Resilient Smart Grid Research Laboratory, Electrical Engineering Department, Azarbaijan Shahid Madani University, Tabriz 5375171379, Iran
[2]Interdisciplinary Centre for Security, Reliability and Trust (SnT), University of Luxembourg, 1359 Luxembourg City, Luxembourg

Corresponding author: S. Najafi Ravadanegh (s.najafi@azaruniv.ac.ir)

This work was supported by the Luxembourg National Research Fund (FNR) LightGridSEED Project, ref. C21/IS/16215802 LightGridSEED. For the purpose of open access, and in fulfilment of the obligations arising from the grant agreement, the author has applied a Creative Commons Attribution 4.0 International (CC BY 4.0) license to any Author Accepted Manuscript version arising from this submission.

ABSTRACT A swift power system restoration in a post-blackout event is one the most important challenges faced by the transmission system (TS) operators (TSO), which is particularly essential in the presence of wind farms, as their potential can be great in a fast restoration. In this study, we propose a bi-level decentralized approach to examine the influence of natural gas network (NGN) constraints on the bulk power system restoration process, taking into account the concurrent effects of pump storage hydropowers (PSHs) and wind farms. At the upper level of the problem, the transmission system (TS) operator (TSO) submits the amount of natural gas fuel consumed by the gas-fired units (GFUs) to the NGN by observing the restoration, operational, and topological constraints. The objective of the TSO is to maximize load servicing in the power grid restoration process. The equilibrium of the proposed bi-level problem is calculated by the analytical target cascading (ACT) algorithm, preserving the privacy of both electricity and NGNs. In the proposed study, an investigation has been conducted into the impact of the gas storage system (GSS) and linepack technology on enhancing the restoration process. Moreover, a moment-based distributionally robust optimization (DRO) approach has been deployed to model the uncertain behavior of wind farms in the restoration process. The proposed approach comprehensively examines the effects of the decentralized interconnection between electricity and NGNs in the restoration process. This facet holds great significance for the advancement of future sustainable energy systems. The results show that ignoring the NGN model leads to 11.92% higher level of unserviced loads.

INDEX TERMS Bi-level decentralized problem, distributionally robust optimization, independent power and natural gas system, linepack technology, power system restoration, privacy preservation.

NOMENCLATURE

Sets and index

t, w	Indices of time period, wind farm.
d, gl	Indices of TS load, NGN load.
i, j	Indices of TS buses.

Parameters

n, m	Indices of NGN nodes.
p	Indices of PSH.
g, r	Indices of power plant, gas producer.
$P_g^{\max}, Q_g^{\max}$	Maximum limits of active (MW), reactive power in units (MVAR).
P_g^{start}	Cranking power of units (MW).
$P_{w,t}^{\max}$	Maximum limit of wind farm (MW).

The associate editor coordinating the review of this manuscript and approving it for publication was S. Ali Arefifar.

$P_d^{\max}$, $Q_d^{\max}$ Maximum limits of restorable active (MW), reactive loads (MVAR).
$G_{g,t}^{D*}$ Gas consumed by GFU (m^3).
α_d Priority factor of load (%).
T_g^{start} Time to start-up the units (p.u).
R_g^{dn}, R_g^{up} Ramp down, ramp up limits in units (MW).
η_g, ϕ Efficiency of GFUs (%), convert factor gas to power in GFUs (%).
η_c, η_d Efficiency of charge/discharge water in PSH (%).
$\underline{H_p}$, $\overline{H_p}$ Maximum and minimum energy storage capacity of PSH (MW).
$\underline{P_p^c}$, $\overline{P_p^c}$ Maximum and minimum energy stored limits of PSH (MW).
$\underline{P_p^d}$, $\overline{P_p^d}$ Maximum and minimum energy discharge limits of PSH (MW).
g_{ij}, b_{ij} Susceptance, conductance in transmission lines.
$\overline{P_{ij,t}^{flow}}$, $\overline{Q_{ij,t}^{flow}}$ Maximum transmission active (MW), reactive power capacity in the TS (MVAR).
$\underline{V_i}$, $\overline{V_i}$ Minimum, maximum limits of bus voltage in TS (KV).
$\underline{\delta_i}$, $\overline{\delta_i}$ Minimum, maximum limits of bus voltage angle in TS.
$P_d^{\max}$ Maximum limit of load pickup (MW).
$G_{g,t}^{D*}$ Target variables for the g th GFU with a fixed value (MW).
$G_{g,t}^{D*}$ Response variables for the g th GFU with a fixed value (MW).
C_r^{Well} Cost of gas producer ($/MW).
C_g^C Cost of selling natural gas fuel to the GFU in TS ($/$m^3$).
$\underline{G_w}$, $\overline{G_w}$ Minimum, maximum limits of natural gas producer (m^3).
$\underline{\Pr_n}$, $\overline{\Pr_n}$ Minimum, maximum limits of NGN nodes pressure (Bar).
$K_{n,m}^f$ The coefficient related to the pipelines of the NGN.
$G_{gl,t}^{Load}$ Residential gas load in NGN (m^3).
$\widehat{\cos}(\delta_{i,t})$ Polyhedral relaxation of $\cos(\delta_{i,t})$.

Variables

$P_{d,t}$, $Q_{d,t}$ Amount of active (MW) and reactive restored load at TS (MVAR).
$G_{g,t}^G$, $G_{g,t}^D$ Response and target variables for the g th GFU.
$P_{p,t}^c$,$P_{p,t}^d$ Charge and discharge in PSH (MW).
$H_{p,t}$ Energy storage capacity of PSH (MW).
$P_{g,t}^{start}$ Startup power of units (MW).
$P_{g,t}$, $Q_{g,t}$ Active (MW) and reactive output power of units (MVR).
$P_{w,t}$ Output power of wind farm (MW).
$P_{ij,t}^{flow}$, $Q_{ij,t}^{flow}$ Active (MW) and reactive power flow in transmission lines (MVAR).
$V_{i,t}$, $\delta_{i,t}$ Voltage of TS bus (KV), Voltage angle bus at the TS (rad).
R_t, $R_{g,t}$ Total dynamic reserve and dynamic reserve share of power units (MW).
$R_{d,t}$ Dynamic reserve share of load shedding (MW).
$R_{w,t}$ Dynamic reserve share of wind farm (MW).
$G_{r,t}^{well}$ Amount of gas producer (m^3).
$\Pr_{n,t}$ Amount of NGN nodes pressure (Bar).
$G_{n,m,t}^{flow}$ Natural gas flow in NGN pipeline (m^3).
$G_{n,m,t}^{in}$, $G_{n,m,t}^{out}$ Inlet and outlet gas flow in NGN (m^3).
$L_{n,m,t}$ Amount of gas stored in NGN pipeline (m^3).

Binary variables

$u_{g,t}^{start}$ Unit start-up status in TS.
$u_{g,t}^{on}$ Unit commitment status in TS.
$u_{w,t}$ Wind farm commitment status in TS.
$u_{l,t}$ Transmission line status.
$u_{i,t}$, $u_{j,t}$ Transmission bus status.

I. INTRODUCTION

The The global consumption of natural gas is predicted to grow by 40% between 2018 and 2050. Meanwhile, it is predicted that the amount of electricity production will reach 25 to 45 trillion kilowatt hours in the same period [1]. The production of electrical energy through gas-fired units (GFU) interconnects electricity and natural gas networks (NGNs). As a result, the operation, reliability, resilience, and restoration of power grids are increasingly reliant on the NGN [2]. Reduced resilience of power systems is one of the basic and important liabilities caused by the increasing dependence of electricity production on the NGN [3]. Accordingly, a proper NGN model should be incorporated into the restoration studies to comprehend its impact. Furthermore, inherent technological advances in the NGN, such natural gas storage systems could be integrated into the problem to observe their outcome in improving the natural gas delivery to the generation units. It is noteworthy that a certain amount of natural gas can be effectively stored in the pipeline itself, which is known as the NGN pipeline, which can be incorporated to expedite the restoration. Therefore, ignoring the inter-dependencies of NGN and power systems can lead to devastating catastrophes. One example of a such contingencies caused by the NGN, is the extensive blackout on 15/2/2021, in the state of Texas, USA [4]. The occurrence of cold and frost in the state of Texas caused an extensive pressure drop in the NGN nodes, and as a result, the production capacity of GFUs decreased drastically. In turn, the gas facilities dependent on electricity (e.g., compressors, valves, and extractors) were shut down due to the widespread power blackout, which led to a sharp shortage in gas provision. Thus, more than 4.8 million

residential consumers were left without gas through deep freeze conditions.

Renewable energy sources can play an important role in reducing dependence of electricity and gas networks due to advantages such as significant reduction in pollution, free resources, and easy operation. It is predicted that by 2050, 50% of electrical energy will be provided by solar and wind energy [5]. In this regard, renewable energy sources can contribute to the restoration of power grids due to their fast start-up and needlessness for cranking power to blackstart. However, most independent system operators are conservative in using renewable energy for system restoration [6]. For example, the independent system operator excludes renewable energy sources from the restoration process and takes them out of service until the final stages of restoration. This conservative attitude is due to the lack of knowledge about the management of variability and the uncertainty of renewable energy in system restoration. However, not using renewable energy sources during the restoration period delays the restoration time and supply of the majority of loads. Therefore, a new restoration strategy for wind or solar-assisted power systems is urgently needed.

Among various storage options, pumped-storage hydro (PSH) stands out as the most mature and economical choice for large-scale applications. PSH units possess the capability to seamlessly switch between pumping and generation modes, offering rapid response energy and reserve capacity. PSH units can quickly switch between pumping (power charging) and generating (power discharging) modes. Therefore, the fast response of PSH units can be a suitable support for the fluctuating behavior of wind farms in the process of restoring power systems. An optimal coordination of wind power and PSH units can minimize the restoration time of power systems [7].

However, in addition to increasing the flexibility of power systems using PSH, it is necessary to accurately model the non-deterministic behavior of fluctuating renewable resources. In this regard, the latest distributionally robust optimization (DRO) schemes have presented a notable efficiency in handling uncertainties, while proving a reasonably conservative solutions. Therefore, it is imperative to observe their impact in improving the availability of the wind energy in the restoration process. It is noteworthy that coordination of these two network needs to be handled with an appropriate decentralized algorithm that ensures a reasonable convergence. To this end, analytical target cascading (ACT) algorithm provides a novel approach for solving such problems, which can also be effective in solving the restoration models

A. LITERATURE REVIEW AND CONTRIBUTIONS

Recently, extensive studies have been conducted on the application of renewable energy sources in the restoration process of power systems. A two-stage stochastic optimization approach is presented in [8] to evaluate the impact of wind farms in the power system restoration process. In this study, the impact of wind farms has been investigated from the location aspect, inertial capability, wind penetration, fluctuations, and uncertainty. To evaluate the coordination of water pump storage units with wind farms in the restoration process of power systems, a two-stage robust optimization approach is proposed in [7]. In the first stage of this study, the starting sequence of the generators is determined, then the load pickup sequence, wind power dispatch level, and pump storage unit operational modes are designated in the second stage. In [9], a risk-based approach has been studied for bulk power systems restoration with high penetration of wind farms. In [10], a two-stage robust optimization algorithm is investigated for the synchronization of power islands under the high penetration of wind farms, considering the bulk power system recovery process. In this study, first, robust distributed restoration models are constructed considering power islands under uncertain conditions. Then a distributed algorithm is developed to solve the problem. In [11], a multi-objective optimization approach has been investigated for the restoration of the power transmission network considering the impact of electric vehicle battery discharge. A propagation-based optimization approach is investigated in [12] for restoring power systems considering the requirements of blackstart resources, power balancing, synchrocheck relays for ties lines and renewable energy sources. A decentralized approach based on distributionally robust optimization (DRO) has been studied in [13] for restoration of transmission and distribution systems under high penetration of wind farms. A mixed integer linear programming (MILP) is investigated in [14] for restoration of electric distribution network (EDN) using distributed generation energy resources. In this study, the goal of the EDN operator is to maximize power supply for critical loads within the network. Study [15] presents a preventive strategy for transmission grid operators that leads to increased resilience of transmission grids against high impact and low probability (HILP) events. In [16], a load restoration program is proposed to improve the resilience of power systems considering the physical constraints of the power network. In this study, benders algorithm is used to solve the proposed problem. In [17], a bi-level optimization framework is presented for power system restoration in the presence of renewable energy sources, electric vehicles, and electric storage systems. At the upper level of this problem, the sequence of generators is determined. Subsequently, the uncertainty of renewable energy sources and electric vehicles is modeled at the lower level problem. An effective two-stage stochastic recovery after storm is investigated in [18] to improve the resilience of microgrids by utilizing mobile emergency resources and network reconfiguration. A mixed integer linear programming is developed in [19] to investigate the coordination of battery storage systems with wind farms in the restoration process of bulk power systems. It is noteworthy that the impact of NGN constraints in power

system restoration has not been addressed in any of the studies [8], [7], [9], [10], [11], [12], [13], [14], [15], [16], [17], [18], [19].

In general, little research has been done on the role of the NGN in blackstart units and the restoration of power systems. Most of the conducted studies focus on the resilience of electricity and NGNs pre or post-disaster. In [20], an optimal dispatch problem of repair crews is investigated to improve the resilience of integrated natural gas and electricity systems. A two-stage robust optimization framework is presented in [21] for integrated electricity and natural gas Transmission systems in the presence of multi-energy systems to increase resilience against natural disasters. In this study, benders algorithm and C&CG were used to solve the two-stage problem. An optimal scheduling has been studied in [22] for the restoration of integrated electricity, natural gas and transportation networks after a HILP event. In this study, alternating direction method of multipliers algorithm is used to solve the proposed problem. In [23], an optimization model is presented for restoration integrated electric and natural gas distribution systems in the presence of mobile emergency energy sources. An optimal multi-objective program is investigated in [24] for restoration of integrated electricity and natural gas distribution networks considering the impact of electrical storage systems. In this proposed program, the island method is used to restoration of electricity and natural gas distribution systems. In [25], a robust two-stage resilient scheduling for the commitment of GFUs in integrated electricity and natural gas distribution systems is proposed to increase resilience in the event of a disaster. A two-stage scheduling has been investigated in [26] to increase the resilience of integrated electricity and natural gas distribution systems by considering the impact of the demand response program. An optimal scheduling framework based-on uncertainty is proposed in [27] to investigate the effect of mobile gas storage systems on the resiliency of the integrated electricity and NGNs. A decentralized robust optimization (RO) approach has been studied in [28] to improve the resilience of independent electricity and natural gas systems considering the N-1 criterion. In this approach, the C&CG algorithm has been used to solve this decentralized problem. An optimal scheduling has been studied in [4] for the restoration of integrated electricity and NGNs considering the time and cost of repair to increase resilience. In [29], a probabilistic optimization approach has been investigated to improve the resilience of integrated electricity and natural gas systems using the demand response program and electric vehicles. In this study, a probabilistic analysis algorithm based-on max-min optimization is used to find the worst scenario of power system outage. In addition to the above studies, much research has been conducted in the field of improving the restoration of bulk power systems. However, in none of the past studies, a decentralized framework based on DRO has been presented to investigate the restoration of independent electricity and natural gas systems under high penetration of wind farms. The main gap of the above studies is summarized as follows.

1) In studies [8], [7], [9], [10], [12], [13], [14], [15], [17], and [19], the authors focus on investigating the impact of using renewable energy sources in the restoration process of power systems. However, the impact of NGN constraints and the application of gas storage systems (GSSs) and linepack technology in the restoration process of power systems have not been scrutinized. For a network where more than 40% of its electricity production is dependent on natural gas fuel, it is obvious that the constraints of the NGN will have a significant impact on the restoration process of the power system.
2) In studies [20], [21], [23], [24], [25], [26], [27], [28], and [29], the authors focus on improving the resilience of integrated electricity and NGNs, and assume that they are operated by a centralized single operator. However, in practice, electricity and NGNs are mostly operated separately in normal and emergency conditions. Hence, they have different operators. Nonetheless, there are also cases in which these two entities are controlled under a single integrated structure, such as currently operational ''PG&E Corporation'' that has undertaken the electricity and natural gas distribution in the northern and central California regions.
3) Except research [13], most authors use stochastic and robust programming to model the uncertain behavior of renewable energy sources. Using the stochastic optimization method can be useful if there are exact probability distribution functions (PDF). However, in practice, either we do not have access to PDFs, or if available, these distributions are not exact. In the RO method, probability distributions are not needed. However, the solution obtained from the RO method is very conservative and leads to imposing additional unnecessary costs on the system operators.

According to the literature review gap and Table 1, the main contribution of this article is summarized as follows:

1) A bi-level decentralized approach is presented to investigate the impact of NGN constraints on the restoration of bulk power systems considering PSH, GSSs and linepack technology and under the high penetration of wind farms. According to the authors' knowledge, this is the first study that investigates the effect of the NGN, GSS and the linepack technology in the restoration process of bulk power systems in a decentralized approach. The proposed approach thoroughly addresses the impact of the interconnection between electricity and natural gas transmission networks in the restoration process. This aspect is crucial for the development of future sustainable energy systems.
2) The analytical target cascading (ATC) algorithm has been used to solve the decentralized optimization

model, which meets privacy requirements between power systems and NGNs.

3) A new moment-based DRO approach is developed to model the uncertain behavior of wind farms in bulk power system restoration. According to the knowledge of the authors, this is the first study on DRO models in the decentralized restoration process of electricity and natural gas systems under the high penetration of wind farms. Solving the proposed problem leads to a distributionally robust solution, which avoids overly conservative results such as the conventional RO method.

In addition to the above contribution, this article tries to answer the following questions:

- What are the effects of electricity network restoration on the NGN, considering 50% production penetration of gas-fired units?
- Can the NGN respond to the heavy demand for GFUs during the restoration period, while supplying the residential consumers?
- What should be done if the power grid restoration time overlaps with the peak hour of the NGN?
- Can the presence of wind farms in the load restoration process, with all its uncertainties, reduce the dependence of electricity production on the NGN?

II. THE DECENTRALIZED OPTIMAL RESTORATION MODEL OF TSO AND GNO (ATC METHOD)

Natural gas is a vital resource for GFU and strongly affects the operation of the power grid in normal and emergency conditions. These generation units depend on stable and reliable supply of natural gas to produce electricity. Fig. 1 shows the interconnection of electricity and NGNs. As is clear, the TS includes conventional power plants, RESs, PSH, sub transmission system loads and distribution system (DS) loads. The NGN also includes gas wells, industrial and residential loads. electricity and NGNs are connected to each other through GFU. In many countries globally, there is a predominant emphasis on preserving the privacy of energy systems, leading to the separate operation of electricity and NGNs. Therefore, improving the coordination of electricity and NGNs under a decentralized optimal approach is very important, especially in critical situations. Hence, this study introduces a decentralized optimization framework utilizing the ATC distributed algorithm. The proposed framework ensures effective coordination between electricity and natural gas systems, particularly in emergency conditions. The details of ATC algorithm are as follows.

The augmented Lagrangian method with a quadratic penalty term is used to relax the set constraints of σ in the model presented in section (IV) [30], as follows:

$$\Phi(\sigma) = v\sigma^T + \left\| w \circ \sigma^T \right\|_2^2 = \sum_{g \in \Omega_{GFU}} (v_g \sigma_g + \left\| w_g \circ \sigma_g \right\|_2^2) \tag{1}$$

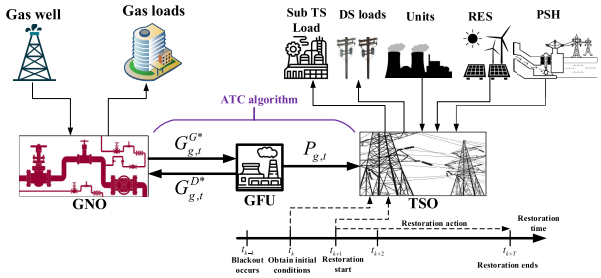

FIGURE 1. Coordination within TS and coordination within NGN.

where v is a Lagrangian coefficient parameter vector, while w is a quadratic term vector. These two vectors are model penalty coefficients and are updated during an iterative process (discussed in Section. IV-D). The symbol $\circ$ also represents the Hadamard multiplier, which shows the entry-wise multiplication of two vectors. Since σ means the distance between the response variable $G^{D*}_{g,t}$ and the target variable $G^{G*}_{g,t}$, the target variables are the only external variables for TSO modeling Eqs. (3)-(41). While the response variable is the only unmanaged variable for each GFU in the NGN Eqs. (42)-(57). Therefore, according to the ATC method, a practical way to manage TSO and GNO external variables is to consider them as parametric values. As shown in Fig. 1, with fixed values of external variables, the coordination of TS and NGN can be easily achieved by decentralized optimization until achieving the point of equilibrium.

III. RESILIENCE INDICES

In general, the time performance of a system against HILP events is shown in Fig. 2. As it is known, in the resilient state (t_0-t_e), the operator tries to identify potential risks and take preventive measures to manage the effects of the future event. Preventive measures can include locations based on equipment resilience, hardening assets, creating redundancy in different parts of power systems. After an event occurs in (t_e-t_{pe}), the power system will lead to equipment damage depending on its resilience level. After the end of the event or disaster in (t_{pe}-t_r), the power system enters the post-event degraded state. Where the resilience of the power system is significantly damaged (the amount of resilience loss of the system is indicated by R_{pe}). At this stage, operators and repairmen should immediately restart the critical part of the power system and put the system in a restoration state. After this stage, the power system enters the restoration state at (t_r-t_{pr}), where the blackstart power plant is start-up and the critical loads are energized. In the next step, the cranking power required by the non-black start units for restarting and the power system enters the post-restoration state. In the post-restoration state (i.e t_{pr}-t_{ir}), the most important part of the power systems has been restored, and the power system can provide the critical loads reliably. In the last step (t_{ir}-t_{pir}), considerable time may pass until the power system reaches the ideal conditions before the event. However, the main focus

TABLE 1. Comparison of the proposed approach with previous studies.

Ref	Network constraints		GSS	Linepack	Algorithm	Uncertainty	Operational resilience	Renewable energy
	Electricity	Gas						
[8]	yes	No	No	No	-	SP	Restoration state	yes
[9]	yes	No	No	No	-	CVaR	Restoration state	yes
[10]	yes	No	No	No	-	RO	Restoration state	yes
[11]	yes	No	No	No	-	-	Restoration state	No
[12]	yes	No	No	No	-	-	Restoration state	yes
[13]	yes	No	No	No	-	DRO	Restoration state	yes
[14]	yes	No	No	No	-	-	Restoration state	No
[15]	yes	No	No	No	-	-	Restoration state	No
[16]	yes	No	No	No	Decentralized	-	Restoration state	No
[17]	yes	No	No	No	-	SP	Restoration state	yes
[18]	yes	No	No	No	-	SP	Restoration state	No
[19]	yes	No	No	No	-	-	Restoration state	yes
[20]	yes	yes	No	No	Centralized	-	Post-event state	No
[21]	yes	yes	No	No	Centralized	RO	Post-event state	yes
[22]	yes	yes	No	No	Decentralized	-	Restoration state	No
[23]	yes	yes	yes	No	Centralized	-	Restoration state	No
[24]	yes	yes	No	No	Centralized	-	Restoration state	No
[25]	yes	yes	yes	No	Centralized	RO	Post-event state	No
[26]	yes	yes	No	No	Centralized	-	Pre/post-event state	No
[27]	yes	yes	yes	No	Centralized	-	Restoration state	No
[28]	yes	yes	No	yes	Decentralized	RO	Pre/post-event state	No
[4]	yes	yes	No	No	Centralized	-	Restoration state	No
[29]	yes	yes	No	No	Centralized	-	Post-event state	yes
This paper	yes	yes	yes	yes	Decentralized	DRO	Restoration state	yes

of this study is on the restoration mode of power systems (ie, t_r-t_{ir}). Therefore, to evaluate the restoration efficiency of the electricity and NGN from $t_r$to t_{ir}, a restoration index (RI) is defined in equation Eq. (2). This index is 100 for a fully efficient system and 0 for a weak system with complete loss of performance.

$$RI = \frac{\int_{t_r}^{t_{ir}} R(t)dt}{(t_r - t_{ir}).R_{pr}}.100 \tag{2}$$

where $R(t)$ represents the studied resilience index. In this study, energizing critical loads and providing cranking power of non-blackstart units in the restoration process of bulk power systems is considered as an indicator. The energization of critical loads is modeled by the key method of weighting or load prioritization, while the cranking power supply of non-black start units is also modeled by constraints of starting generators.

IV. MATHEMATICAL MODELING

A. TRANSMISSION SYSTEM RESTORATION MODEL (UPPER LEVEL)

The objective function of the transmission system operator (TSO) is expressed in Eq. (3). As it is known, the first and second terms of Eq. (3) respectively express the maximization of the total generation power of conventional generators and wind units. The third term is the objective function of minimizing the unserved loads during the restoration period of power systems. The fourth and fifth terms also express the penalty of the ATC algorithm to achieve convergence between the problems of the power and NGNs.

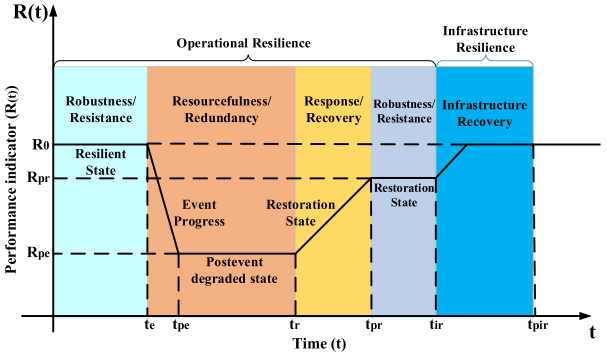

FIGURE 2. Power system resilience curve.

$$\max \sum_{t} \left\{ \begin{array}{l} \sum_{g} \left(P_g^{\max} - P_g^{start} \right) u_{g,t}^{on} + \sum_{t} \sum_{w} P_{w,t}^{\max} u_{w,t} \\ - \sum_{t} \sum_{d} \alpha_d \left(P_d^{\max} - P_{d,t} \right) - \\ \sum_{g \in GU} \nu_g \left(G_{g,t}^{G} - G_{g,t}^{D*} \right) + \left\| w_g \circ \left(G_{g,t}^{G} - G_{g,t}^{D*} \right) \right\|_2^2 \end{array} \right\} \tag{3}$$

The binary variable $u_{g,t}^{on}$ expresses the generation status of unit g at the restoration time t, while $P_g^{\max}$ and P_g^{start} represent the generation capacity and cranking power of the units, respectively. In addition, α_d expresses the load priority

coefficient,$P_d^{\max}$ indicates the maximum restorable load, and $P_{d,t}$ is the total restored load during the time period t.

1) CONSTRAINTS OF INITIAL CONDITIONS

Before running the optimization problem, the TSO must determine the initial state of the TS following a blackout. The main infrastructure of the power grid can suffer extensive damage from natural disasters. Therefore, some network components may not be immediately available for restoration after a blackout. On the other hand, the occurrence of some incidents, such as cyber-attacks targeting substations, power plants, or local facilities, is considered, which may cause partial blackout. In such cases, the major part of the network is not affected and does not require major restoration measures. In this paper, it is assumed that a complete blackout occurs without causing serious damage to the network equipment as well as the main infrastructure of the system. Conventional generating units as well as wind turbines are readily available to help restore the power grid. Therefore, it is easy to set the constraints of the problem with initial conditions. Eqs. (4)-(5) indicate that at $t = 0$, all non-blackstart units are off, and transmission lines/buses are not energized. Eq. (6) shows that the network restoration process starts at $t = 1$ when the black start units [1] are turned on [8].

$$u_{g,t=0}^{\text{start}} = 0 \quad \forall g \in G_{NBSU} \tag{4}$$

$$u_{l,t=0} = 0 \quad u_{n,t=0} = 0 \tag{5}$$

$$u_{g,t=1}^{\text{start}} = 1 \quad \forall g \in G_{BSU} \tag{6}$$

2) FUNCTIONS OF STARTING GENERATORS

The starting characteristic of non-blackstart units is shown in Eq. (7). As it is known, Eq. (7) is a nonlinear equation, the details of its linearization are presented in [31].

$$P_{g,t}^{start} = \begin{cases} 0 & 0 \le t \le t_g^{start} \\ P_g^{start} & t_g^{start} \le t \le t_g^{start} + T_g^{start} \end{cases} \tag{7}$$

Restarting the units and re-energizing the transmission lines are necessary for the restoration process. Eq. (8) indicates that it is necessary to start the non-blackstart units that the bus bg has energized. Assuming that a transmission line l connects buses n and m, if both buses are cut off at restoration time t, transmission line l remains de-energized at time t in equation Eq. (11) [32].

$$u_{g,t}^{start} \le u_{i,t} \quad \forall i \in A_b^i, \ \forall g, \ \forall t \tag{8}$$

$$\sum_t (1 - u_{g,t}^{on}) \ge \sum_t (1 - u_{g,t}^{start}) + T_g^{start} \quad \forall g \tag{9}$$

$$u_{w,t} \le u_{i,t}, \quad \forall i \in A_i^w, \ \forall w, \ \forall t \tag{10}$$

$$u_{l,t} \le u_{i(j),t} \ \forall l \in A_j^i, \ \forall ij, \ \forall t \tag{11}$$

$$u_{l,t+1} \le (u_{i,t} + u_{j,t}) \quad \forall l \in A_j^i, \ \forall ij, \ \forall t \tag{12}$$

3) GENERATOR CHARACTERISTIC LIMITATIONS

Eqs. (13)-(14) expresses the limitation of active and reactive power generation of TS generators, respectively. Eq. (15) has also been to model the constraints of the forecasted wind power. Eqs. (17)-(24) show the constraints of the active and reactive ramp rate power of production units. Eq. (24) shows the coupling of the electricity TS to the NGN through GFUs [33].

$$P_g^{\min} u_{g,t}^{on} \le P_{g,t} \le P_g^{\max} u_{g,t}^{on} \quad \forall g, \ \forall t \tag{13}$$

$$Q_g^{\min} u_{g,t}^{on} \le Q_{g,t} \le Q_g^{\max} u_{g,t}^{on} \quad \forall g, \ \forall t \tag{14}$$

$$0 \le P_{w,t} \le P_{w,t}^{\max} u_{w,t} \quad \forall w, \ \forall t \tag{15}$$

$$R_g^{dn} \le P_{g,t} - P_{g,t+1} \le R_g^{up} \quad \forall g, \ \forall t \tag{16}$$

$$R_g^{dn} \le Q_{g,t} - Q_{g,t+1} \le R_g^{up} \quad \forall g, \ \forall t \tag{17}$$

$$G_{g,t}^G = \phi P_{g,t} \tfrac{1}{\eta_g} \quad \forall g, \ \forall t \tag{18}$$

4) CONSTRAINTS OF PUMPED STORAGE HYDROPOWER

The operation constraints of the PSH are modeled through Eqs. (19)-(23). Eq. (19) expresses the way of energy storage by PSH. The capacity limitation of the PSH is also expressed through Eq. (20). The charging and discharging limitations of the PSH storage system are modeled through Eq. (21) and Eq. (22), respectively. Eq. (23) also prevents simultaneous charging and discharging in the network restoration process [7].

$$H_{p,t} = H_{p,t-1} + \eta_c P_{p,t}^c - P_{p,t}^d \Big/ \eta_d \tag{19}$$

$$\underline{H_p} \le H_{p,t} \le \overline{H_p} \tag{20}$$

$$Z_{p,t}^c \underline{P_p^c} \le P_{p,t}^c \le Z_{p,t}^c \overline{P_p^c} \tag{21}$$

$$Z_{p,t}^d \underline{P_p^d} \le P_{p,t}^d \le Z_{p,t}^d \overline{P_p^d} \tag{22}$$

$$Z_{p,t}^d + Z_{p,t}^c \le 1 \tag{23}$$

5) CONSTRAINTS OF POWER FLOW AND POWER BALANCE

Eqs. (24)-(25) express the active and reactive power balance equations in the TS, respectively. Eqs. (26)-(27) are modeled active and reactive power flow in the TS. Active and reactive power flow in the TS are modeled in Eqs. (26)-(27). The power flow proposed in this paper is linearized using the method presented in [34]. Eqs. (28)-(29) express the limits of active and reactive power that can be transmitted in power grid lines. Voltage and bus angle limits in the TS are also modeled through Eqs. (30)-(31).

$$\sum_{g \in A_i^g} (P_{g,t} - P_{g,t}^{start}) + \sum_{w \in A_i^w} P_{w,t} - \sum_{d \in A_i^d} P_{d,t} + \sum_{p \in A_i^p} (P_{p,t}^d - P_{p,t}^c) = \sum_{j \in A_i^j} P_{ij,t}^{flow} \quad \forall i, \ \forall t \tag{24}$$

$$\sum_{g \in A_i^g} Q_{g,t} + \sum_{w \in A_i^w} Q_{w,t} - \sum_{d \in A_i^d} Q_{d,t} = \sum_{j \in A_i^j} Q_{ij,t}^{flow} \quad \forall i, \ \forall t \tag{25}$$

$$P_{ij,t}^{flow} = g_{ij}(V_{i,t} - V_{j,t} - \widetilde{\cos}(\delta_{i,t}) + 1) - b_{ij}(\delta_{i,t} - \delta_{j,t}) \quad \forall ij, \ \forall t \tag{26}$$

[1] A black start unit does not require initial electricity for start-up

$$Q_{ij,t}^{flow} = -b_{ij}(V_{i,t} - V_{j,t} - \widetilde{\cos}(\delta_{i,t}) + 1) - g_{ij}(\delta_{i,t} - \delta_{j,t}) \quad \forall ij,\ \forall t \tag{27}$$

$$-\overline{P_{ij,t}^{flow}} \le P_{ij,t}^{flow} \le \overline{P_{ij,t}^{flow}} \quad \forall ij,\ \forall t \tag{28}$$

$$-\overline{Q_{ij,t}^{flow}} \le Q_{ij,t}^{flow} \le \overline{Q_{ij,t}^{flow}} \quad \forall ij,\ \forall t \tag{29}$$

$$\underline{V_i} \le V_{i,t} \le \overline{V_i} \quad \forall i,\ \forall t \tag{30}$$

$$\underline{\delta_i} \le \delta_{i,t} \le \overline{\delta_i} \quad \forall i,\ \forall t \tag{31}$$

6) CONSTRAINTS OF COLD PICKUP LOADS

In load restoration, it should be noted that when a large load is picked up, a severe frequency drop occurs, which leads to instability in the entire power system. In this approach, a load restoration coefficient is defined for each production unit. In other words, the coefficient of each load is calculated as the maximum load that a generator can supply without causing a frequency drop. These load restoration coefficients are calculated for 5% of fossil-fueled units, 15% hydro units, and 25% combustion units [7]. Loads of the TS can be restored as soon as the corresponding buses are energized, which is modeled by Eq. (32). The maximum cold pickup load capability is also calculated by Eq. (34) [33].

$$0 \le P_{d,t} \le P_d^{\max} u_{i,t} \quad \forall i \in A_i^d,\ \forall d,\ \forall t \tag{32}$$

$$\sum_d P_{d,t+1} - \sum_d P_{d,t} \le \sum_g R_{g,t} \quad \forall t \tag{33}$$

$$R_{g,t} \le \min(P_g^{\max}\lambda_g, P_g^{\max} - P_{g,t}) \quad \forall g,\ \forall t \tag{34}$$

Equation (29) shows the total dynamic reserve of the power system in the network restoration process. It is worth noting that UFLS according to practical procedures should be 50% less than the total system reservation, which is modeled by Eq. (36).

7) DYNAMIC RESERVATION CONSTRAINTS

Dynamic reservation constraints are applied to ensure system stability. Especially when contingencies occur, the frequency of the system must be kept within an acceptable range. The Eq. (35) shows the dynamic reserve of the power system in the network restoration process. As is clear, dynamic reservation is obtained from three sources of reservation including conventional generating units, wind units and under frequency load shedding (UFLS). It is worth noting that UFLS according to practical procedures should be 50% less than the total system reservation, which is modeled by Eq. (36). If we assume that R_t represents the reservation level at time t, the dynamic reservation constraints are calculated as follows [8].

$$R_t \le \sum_{d\in D} R_{d,t} + \sum_{g\in G} R_{g,t} + \sum_{w\in W} R_{w,t} \quad \forall t \tag{35}$$

$$\sum_d R_{d,t} \le 0.5R_t \quad \forall t \tag{36}$$

For each of the energy sources, including wind farms and conventional production units, the dynamic reserve should be limited based on their available capacity. For this purpose, Eqs. (37)-(38) apply the upper limit of the dynamic reserve for conventional production units and wind farms. Eq. (39) relates the maximum dynamic reserve available to the governor characteristics of power plants. Where, variable ΔP_g shows the load pickup of generators, which can be calculated using Eq. (34) [8].

$$R_{g,t} \le P_g^{Max} - P_{g,t} \quad \forall g,\ \forall t \tag{37}$$

$$R_{w,t} \le P_{w,t}^{Max} - P_{w,t} \quad \forall w,\ \forall t \tag{38}$$

$$R_{g,t} \le \Delta P_g \quad \forall g,\ \forall t \tag{39}$$

To deal with the loss of large production units, we must make sure that the active power of conventional generators and wind generators does not exceed the total dynamic reserve of the system [8].

$$P_{g,t} \le R_t - R_{g,t} \quad \forall g,\ \forall t \tag{40}$$

$$P_{w,t} \le R_t - R_{w,t} \quad \forall w,\ \forall t \tag{41}$$

B. NGN MODELING (LOWER LEVEL)

The NGN is modeled through Eqs. (42)-(57) based on the SOCP relaxation method [25]. Eq. (42) expresses the objective function of the NGN. The first term is the objective function expressing the production minus the sale of natural gas to the power grid. Moreover, the second term of the equation expresses penalty term of the ATC algorithm. The constraints of natural gas production and pressure of NGN nodes are modeled through equations Eqs. (43)-(44) respectively. Eq. (45) expresses the gas flow in the NGN (Weymouth equation). As it is known, Eq. (45) is a non-linear and non-convex equation. Therefore, Eq. (45) is relaxed into Eq. (46) to benefit from the computational advantages of SOCP. The natural gas flow is modeled by Eq. (47) considering linepack technology. Eq. (48) expresses the direct relationship between the linepack technology and pressure level in NGN nodes. Eqs. (49)-(50) also indicate the level of natural gas stored in pipelines. Eq. (51) models the initial storage value of the linepack system. The amount of stored natural gas in GSS is established via Eq. (52), whilst Eqs. (53)-(55) limit the charge/discharge rates and the amount of stored natural gas within the nominal degrees. Similar to the other storage units, the initial and final storage statues are equalized by Eq. (56) to hold up the energy conservancy. Eventually, The NGN balance equation is also modeled through Eq. (57) [35].

$$\min \sum_t \left\{ \begin{array}{l} \sum_{\mathrm{r}} C_{\mathrm{r}}^{\mathrm{Well}} G_{\mathrm{r,t}}^{\mathrm{well}} - \sum_{\mathrm{g}\in\mathrm{GU}} C_{\mathrm{g}}^{\mathrm{C}} G_{\mathrm{g,t}}^{\mathrm{D}} \\ -\sum_{\mathrm{g}\in\mathrm{GU}} \nu_{\mathrm{g}} \left(G_{\mathrm{g,t}}^{\mathrm{D}} - G_{\mathrm{g,t}}^{\mathrm{G}^*}\right) \\ + \left\| w_{\mathrm{g}} \circ \left(G_{\mathrm{g,t}}^{\mathrm{D}} - G_{\mathrm{g,t}}^{\mathrm{G}^*}\right) \right\|_2^2 \end{array} \right\} \tag{42}$$

$$\underline{G_w} \le G_{r,t}^{well} \le \overline{G_w} \quad \forall r,\ \forall t \tag{43}$$

$$\underline{\mathrm{Pr}_n} \le \underset{n,t}{\mathrm{Pr}} \le \overline{\mathrm{Pr}_n} \quad \forall n,\ \forall t \tag{44}$$

$$(G^{flow}_{n,m,t})^2 = K^f_{n,m}(Pr^2_{n,t} - Pr^2_{m,t}) \quad \forall n, \forall m, \forall t \tag{45}$$

$$\left\| \begin{matrix} G^{flow}_{n,m,t} \\ K^f_{n,m} Pr_{m,s,t} \end{matrix} \right\|_2 \leq K^f_{n,m} Pr_{n,t} \quad \forall n, \forall m, \forall t \tag{46}$$

$$G^{flow}_{n,m,t} = \frac{G^{in}_{n,m,t} - G^{out}_{n,m,t}}{2} \quad \forall n, \forall m, \forall t \tag{47}$$

$$L_{n,m,t} = C^f_{n,m} \frac{Pr_{n,t} + Pr_{m,t}}{2} \quad \forall n, \forall m, \forall t \tag{48}$$

$$L_{n,m,t} = L_{n,m,t-1} + G^{in}_{n,m,t} - G^{out}_{n,m,t} \quad \forall n, \forall m, \forall t \geq 1 \tag{49}$$

$$L_{n,m,t} = L_{n,m,0} + G^{in}_{n,m,t} - G^{out}_{n,m,t} \quad \forall n, \forall m, \forall t = 1 \tag{50}$$

$$L_{n,m,t} \leq L_{n,m,0} \quad \forall n, \forall m, \forall t \tag{51}$$

$$GS^{GSS}_{h,t} = GS^{GSS}_{h,t-1} + \eta^{GSS,ch}_h G^{ch}_{h,t} - \frac{G^{dis}_{h,t}}{\eta^{GSS,dis}_h} \quad \forall h, \forall t \tag{52}$$

$$0 \leq G^{ch}_{h,t} \leq GS^{ch,\max}_h, \forall h, \forall t \tag{53}$$

$$0 \leq GS^{dis}_{h,t} \leq GS^{dis,\max}_h, \quad \forall h, \forall t \tag{54}$$

$$GS^{Min}_h \leq GS^{GSS}_{h,t} \leq GS^{Max}_h, \quad \forall h, \forall t \tag{55}$$

$$GS_{h,t=0} = GS_{h,t=24}, \forall h, \quad \forall t \tag{56}$$

$$\sum_{r \in A^r_n} G^{well}_{r,t} - \sum_{gl \in A^{gl}_n} G^{Load}_{gl,t} - \sum_{g \in A^g_n} G^D_{g,t} - \sum_{h \in A^h_n} G^{ch}_{h,t} + \sum_{h \in A^h_n} G^{ds}_{h,t} = \sum_{m \in A^m_n} (G^{in}_{n,m,t} - G^{out}_{m,n,t}) \forall n, \forall t \tag{57}$$

C. MATHEMATICAL MODELING OF DRO

The stochastic optimization model does not provide a robust behavior in its solution and requires exact probability distribution functions $\pi = \{\pi_s, \forall s \in \Omega\}$ for scenario generation, which may not be feasible in many situations. On the other hand, the RO method is overly conservative and leads to imposing additional costs on the operators [36]. Therefore, we have proposed a DRO framework to model the uncertain behavior of the wind farms in the TS. The solution of the proposed approach leads to the presentation of a robust solution, which avoids overly conservative solutions, such as the conventional robust optimization method. In the DRO approach, instead of minimizing the expected value in the worst case, the expected value by worst-case probability distribution in the ambiguity set $\mathfrak{D}$ to an estimated distribution $\mathbb{P}_\xi$ is minimized. Eq. (58) is a conventional formula of the ambiguity set $\mathfrak{D}$ that considers all possible distributions with mean vector μ and standard deviation matrix σ [37].

$$\mathfrak{D} = \left\{ \mathbb{P}_\xi \in M^M_+ \middle| \begin{matrix} \mathbb{P}\{\xi \in \Xi\} = 1 \\ (\mathbb{E}_\mathbb{P}\{\xi\} - \mu)^T \sigma^{-1} (\mathbb{E}_\mathbb{P}\{\xi\} - \mu) \leq \Gamma_1 \\ \mathbb{E}_\mathbb{P}\left\{(\xi - \mu)(\xi - \mu)^T\right\} \leq \Gamma_2 \sigma \end{matrix} \right\} \tag{58}$$

where M^M_+ represents the set of all valid probability distributions in $\mathbb{R}^M$. Additionally, $\mathbb{P}\{\xi \in \Xi\} = 1$ is called the support set, which has the purpose of realizing the uncertainties in a limited set Ξ. In addition, $\Gamma_1 \geq 0$ and $\Gamma_2 \geq 1$ are uncertainty control parameters, whose task is to control the volume of the ambiguity set. In this way, it is possible to reformulate the DRO problem for wind farms in the TS by equation Eq. (59).

$$OF_1 = \min \max_{\mathbb{P} \in \mathfrak{D}} \sum_t \mathbb{E}_\mathbb{P} \left\{ \begin{matrix} \sum_g \left(P^{start}_g - P^{\max}_g\right) u^{on}_{g,t} \\ - \sum_t \sum_w P^{\max}_{w,t} u_{w,t} + \\ \sum_t \sum_d \alpha_d \left(P^{\max}_d - P_{d,t}\right) \\ + \sum_{g \in GU} \nu_g \left(G^G_{g,t} - G^{D*}_{g,t}\right) \\ + \left\| w_g \left(G^G_{g,t} - G^{D*}_{g,t}\right) \right\|^2_2 \end{matrix} \right\} \tag{59}$$

s.t Eqs. (4)-(36)

Eq. (59) is in general a bi-level problem, which cannot be solved by conventional commercial solvers. To this end, we convert the min-max problem into a min-min problem using the theory of duality. The details of this duality conversion method are fully presented in [38].

D. INTERACTION BETWEEN GNO AND TSO BY ATC ALGORITHM

Fig. 3 shows the interaction process of GNO with TSO under the ATC iterative algorithm. The interaction between GNO and TSO is done through the exchange of boundary information between TS and NGN. Boundary information refers to the boundary power value calculated by TSO and GNO. Although the objectives of TS and NGN are different, with the presented algorithm, they can have a significant impact on each other. The inner loop shows the interaction between GNO and TSO and the outer loop updates the penalty coefficients. In each iteration, TSO and GNO independently determine their strategies by Eqs. (3)-(41) and Eqs. (42)-(57), respectively. In this algorithm, after running the restoration strategy program, the TSO calculates the amount of natural gas fuel demand of GFU units (i.e., $G^{G*}_{g,t}$ value) and submits it to GNO as a parameter. On the other hand, GNO receives the values of natural gas fuel demand of GFU units (i.e. value $G^{G*}_{g,t}$) and sends this value back to TSO again after implementing optimal dispatch scheduling. This process continues until both systems reach an equilibrium point (or the convergence criterion is satisfied) [30].

V. SIMULATION AND RESULTS

The coordination of electricity and NGN topology is presented in Fig. 4. As it is known, the electricity and NGN are connected to each other through GFUs. In the proposed problem, the power transmission system is simulated by IEEE 57-bus standard test system. Additionally, the NGN has been modeled using the real-world Belgian 20-node

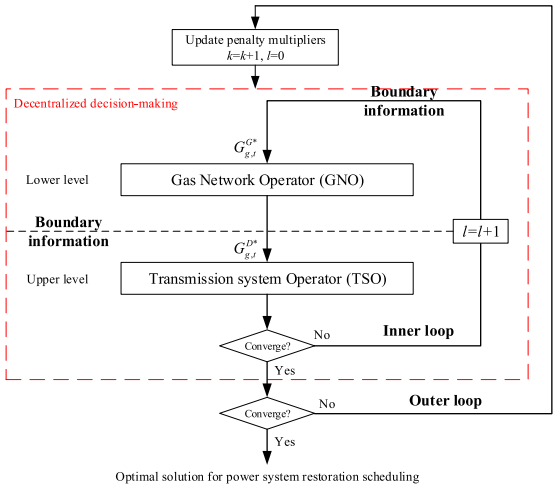

FIGURE 3. Interaction between TSO and GNO by the ATC iterative algorithm.

TABLE 2. Solution time of case study's.

Case study	Solution time (Second)
Case study 1-A	321
Case study 1-B	356
Case study 2-A	2125
Case study 2-B	2413
Case study 2-C	2759
Case study 3	2896

network. Information and data related to TS and natural NGN can be accessed through the link provided in [39]. The expected value of the wind farms are plotted in Fig. 5 In the proposed TS, the total amount of de-energization is 1250.5 MW. In this modeling, the G1 unit is defined as a blackstart unit and the rest of the power plants are defined as non-blackstart units. Moreover, the configuration includes two wind farms, each boasting a capacity of 100 MW and situated at buses 37 and 42. Additionally, two PSH units, with a maximum capacity of 300 MW, have been strategically positioned at buses 38 and 56. Comprehensive details and data regarding the PSH installations can be found in Appendix B. The specifications and types of generators are presented in Table 2. Each step of network restoration time is 10 minutes (1p.u), which is required for preparation and frequency stabilization. In the proposed approach, the wind farm is operated with a unit power factor. The proposed approach is a MILP which is simulated in the GAMS programming environment and solved with a powerful CPLEX solver. The built model is implemented in a personal laptop with hardware features Intel(R) Core(TM) i5-8250U CPU @ 3.50 GHz (4 CPUs) and 8 GB of RAM. In addition, the solution time of the different case studies is presented in table. 2.

1) CASE STUDY 1-A

In the first case study, the effect of wind farms in the restoration process of the TS is investigated. In this case study,

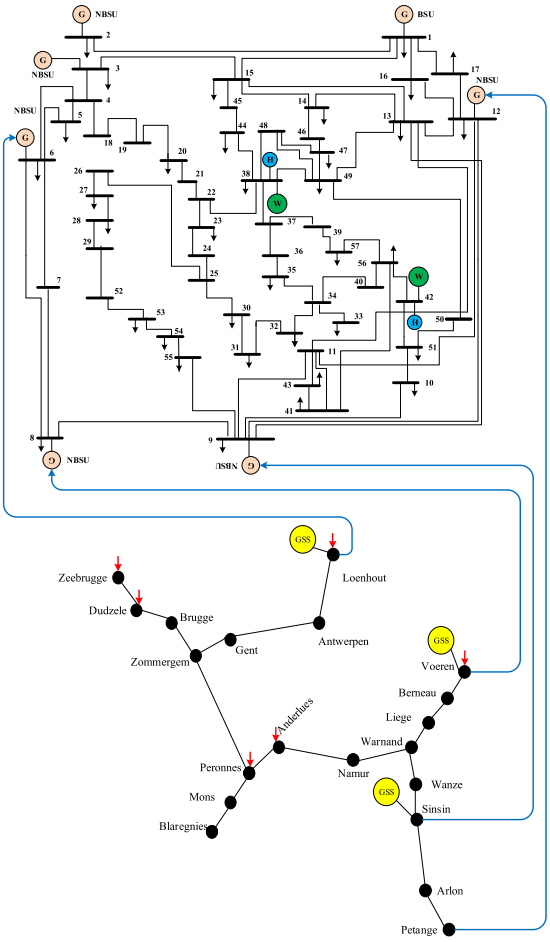

FIGURE 4. Coordinated electricity and NGN topology.

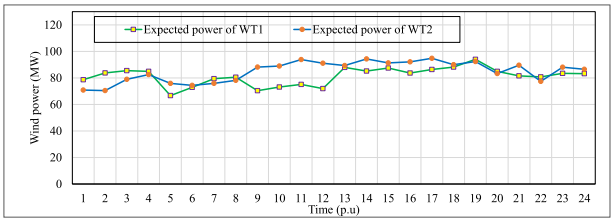

FIGURE 5. Foretasted expected value if the wind farms.

the constraints of the NGN have not yet been considered. Fig. 6 shows the restoration process of the TS with/without consideration of wind farms. Table 3 also shows the start-up time of the power plants. As it is known, the start-up time of blackstart unit G1 is t=3 (p.u). Accodingly, the first bus is energized at time t=3 (p.u) and the restoration process begins. At the next stage, the first non-blackstart unit is synchronized with the power grid at t=12 (p.u). The continuous red graph in Fig. 6 shows the load restoration process without considering the wind farm.

As it is shown, (from Fig. 6), the restoration process started at time t=3 (p.u) and ends at time t=19 (p.u). The total restored active power without considering wind farms is

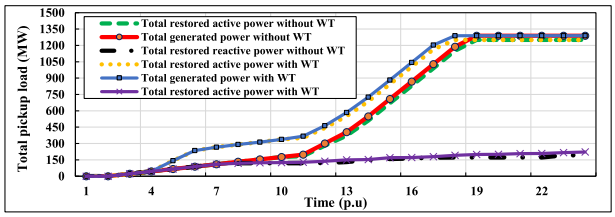

FIGURE 6. Restoration process with/ without wind farms.

TABLE 3. Type and start-up time of the generation units.

Type of unit	Time (p.u)	Unit
Hydro unit	3	G1
NGFU	14	G2
NGFU	13	G3
GFU	11	G4
GFU	11	G5
GFU	12	G6
GFU	13	G7

2213.1 MWh. In addition, the total generation capacity of TS units without considering wind farms is 2294.56 MWh. The blue dashed graph in Fig. 6 shows the load restoration process considering the impact of wind farms. The wind farms in busses 38 and 42 start producing electric power at times $t = 6$ and $t = 5$, respectively. It is worth mentioning that in this study, the uncertain behavior of wind farms is modeled by SP. The total restored power in the presence of wind farms is 2575.093 MWh, which is 361.995 MWh more than the previous state (i.e. without the presence of wind farms). In addition, the load restoration time is reduced by 1(p.u) compared to the previous state. Therefore, it can be concluded that the presence of wind farms in the load restoration process leads to a speedy restoration, improvement of pickup load and increasing the resilience of the TS. The Fig. 7 shows the order of energization of electricity transmission network loads in this case study. As it is known, after starting the black start generator at $t = 3$, part of the critical loads 19, 23, 24 and 26 are energized in order of priority. In the next steps, by increasing the production power of the blackstart generator and start-up other generators, the remaining loads are also energized. Similarly, Fig. 8 shows the scheduling of power system loads coming online during the restoration period. As it is known, the yellow color indicates the time of energizing the loads of the power system.

2) CASE STUDY 1-B

In this case study, the effect of the presence of pumped storage hydropower unit (PSH) in the restoration process of power systems is investigated. For this purpose, two PSHs of power systems have been placed in buses 42 and 53. the sensitivity analysis of the restoration process for the total network loads under various PSH initial values is illustrated in Fig. 9. As it is known, the amount of restored loads is significantly dependent on the initial value of PSH (the capacity of PSH before blackout). In other words, the more energy stored

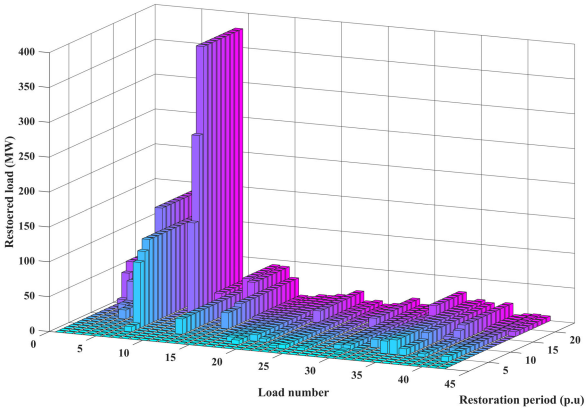

FIGURE 7. The process of energizing loads during the power grid restoration period.

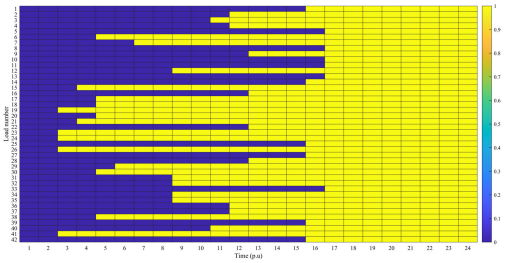

FIGURE 8. Optimal scheduling of power grid loads coming online during the restoration period.

in the PSH before the blackout, the more the restored load increases. In addition, the restoration process with/without considering PSH is also compared in Fig. 9. As it is known, the presence of PSH can reduce the unserved loads in the restoration process of power systems.

Similarly, Fig. 10 shows the online scheduling of power system loads in the restoration time period, where the upward slope of the line represents storage and the downward slope of the line represents energy discharge. As it is known, PSH is started at time t=5 p.u and starts to store or discharge electrical energy compared to the initial capacity. For example, in the case of A0=22MW, the PSH starts to store electrical energy at times t=5 to t=10 (because the initial value of PSH is low) and then starts discharging electrical energy to the grid from time t=11 onwards. On the other hand, in the case of A0=250 MW, due to the high value of the initial capacity, the PSH starts to discharge electrical energy immediately after restarting at t=5 and significantly improves the network restoration.

3) CASE STUDY 2-A

In this case study, the impact of NGN constraints on the restoration process of the TS under the proposed ATC algorithm is investigated.

Fig. 11 shows the load restoration process considering the constraints of the NGN. The continuous graph line in Fig. 11 shows the load restoration process in the presence of NGN

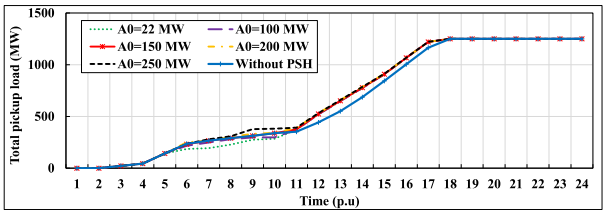

FIGURE 9. Sensitivity analysis of load restoration process for initial values of PSH storage.

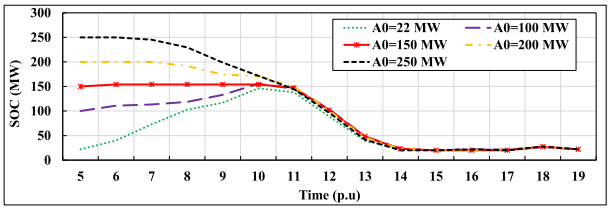

FIGURE 10. Optimal scheduling of PHS system storage for different initial values.

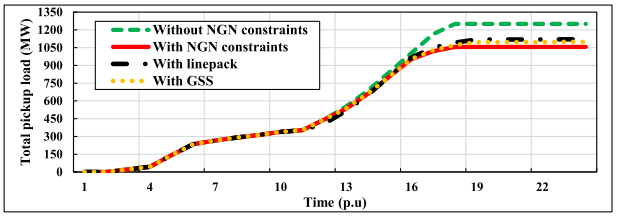

FIGURE 11. Impact of NGN constraints on the TS restoration process.

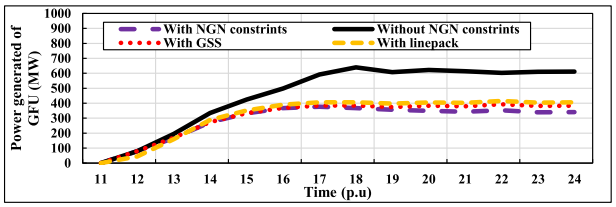

FIGURE 12. Total generation power of GFUs with/without considering the constraints of the NGN.

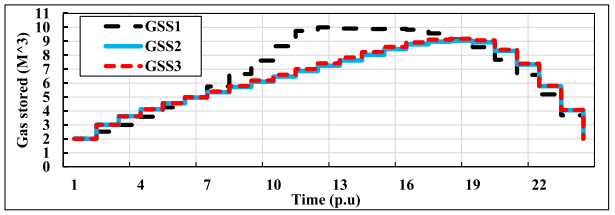

FIGURE 13. Charge and discharge patterns of the GSS.

constraints. The total restored power in the presence of NGN constraints is 2301.35 MWh, which is 273.74 MWh less than case study 1. The reason for the reduction in the total restored power is that the priority of supplying residential loads in the NGN is higher than supplying industrial loads (like the GFUs' gas demand). In addition, the presence of pressure constraints in the NGN nodes, and gas flow constraints in the pipeline cause limitations on fuel supply to GFUs. Therefore, it is clear from Fig. 11 that the area under the curve is significantly smaller when NGN model is considered, which means that less power demand is restored. In this regard, it is obvious that ignoring the NGN model can result in destructive overestimation of the actual production capacity. Fig. 12 shows the total generation power of GFUs with/without considering the constraints of the NGN. The total production power of GFUs without/with the NGN constraints is 1071.64 MWh and 674.34 MWh, respectively. Consequently, the presence of NGN constraints curtails the total production capacity of GFUs decreases by 397.30 MWh.

4) CASE STUDY 2-B

In this case study, the impact of using the GSS in the load restoration process is investigated. Fig. 12 shows the effect of using the GSS (pay attention to the yellow dashed graph). To check the application of GSSs in the network restoration process, three GSSs are connected in nodes 5, 6, and 7 of the NGN. The capacity of each GSS is 10 million cubic meters. The total restored power in the presence of the GSS is 2347.05 MWh, which is 45.69 MWh more than the case without GSS. In addition, the total production power of GFUs is 714.42 MWh, which is 40.425 MWh more than the case without GSS. The scheduled charge/discharge patterns of the GSS is shown in Fig. 13. As it is illustrated, the GSS starts to store natural gas in the reservoirs at the initial time steps of restoration and starts to discharge in the final time steps. This phenomenon reduces the fuel-supply limitation to GFUs in the restoration process.

5) CASE STUDY 2-C

In this case study, the impact of using linepack technology in the load restoration process is evaluated. The black dashed graph in Fig. 11 shows the load restoration process in the presence of linepack technology. The total restored power in the presence of linepack technology is 2368.13 MWh, which is 66.78 MWh more than the case without linepack technology. Furthermore, the total production power of GFUs is 742.92 MWh, which is 71.92 MWh more than the case without linepack technology. Fig. 14 shows how linepack technology is stored in NGN pipelines. As it is demonstrated, natural gas is stored in the pipeline at the beginning of restoration and injected back into the network at the final time steps. In general, the use of linepack technology has led to an increase in fuel supply to GFUs and thus improves the network restoration process. However, a power grid where 50% of its units are GFU can create high stress in the NGN. In this study, even considering all the flexible resources (such as GSS and linepack technology), gas network constraints prevents the full restoration of the TS. Thus, in power grids where the production of electric energy is highly dependent on natural gas fuel, it is very necessary to model the limitations of the NGN in the restoration process.

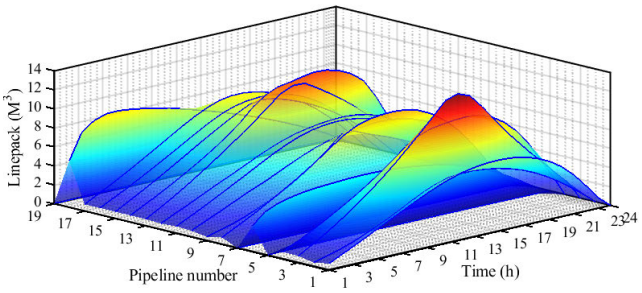

FIGURE 14. The linepack storage level in different NGN pipes.

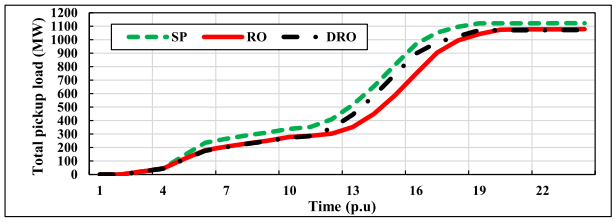

FIGURE 15. The restoration process of coordinated natural gas and electricity networks under different uncertainty strategies.

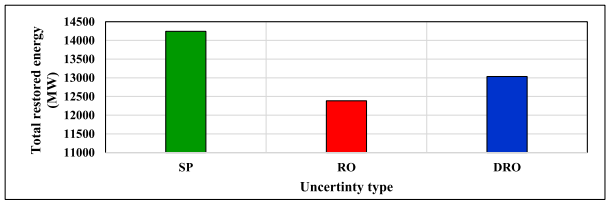

FIGURE 16. Total restored power of the power grid under different uncertainty strategies.

6) CASE STUDY 3

In this case study, the effect of uncertain behavior of wind farms in the restoration process of electricity and NGNs is investigated in the framework of DRO. Fig. 15 shows the restoration process of coordinated natural gas and electricity networks under different uncertainty strategies. As it is clear from this figure, the DRO method provides an intermediate solution compared to the usual stochastic and robust optimization methods. Fig. 16 presents the total restored power of the power grid under different uncertainty strategies. In the SP and RO approaches, the total restored power is calculated as 2373.85 MWh and 2063.98 MWh, respectively. While the total power restored in the DRO strategy is 2172.31 MWh. However, the SP strategy has no robustness in the worst case scenarios, and it requires a great number of SP scenarios to capture the PDFs. On the other hand, the RO method provides the lowest restored load. Therefore, the RO method has high robustness in the worst case. But still, it may lead to increased unserved load in the network restoration process and slow down the restoration. The solution provided by the DRO optimization strategy, while compensating the robustness of the SP method, avoids the overly conservative solutions of the RO. It should be noted that the convergence of the ATC algorithm under different uncertainty strategies has been proven in Fig. 17.

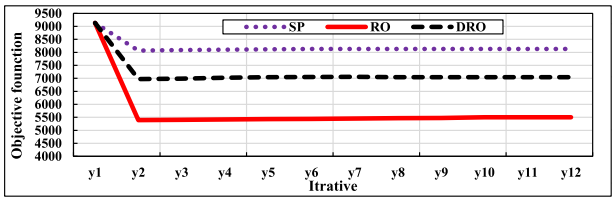

FIGURE 17. Convergence of the ATC algorithm under different uncertainty strategies.

VI. DISCUSSION

As it was noted, the study was implemented in three case studies. The first study case was examined in two subsections. The first sub-case illustrates how wind farms could impact the restoration process, which showed that they can augment the restored loads by 2575.09 MWh. In the second sub-case study, the coordination of PSH and wind farm was investigated in the process of restoring power systems. The obtained results show that the presence of PSH leads to a reduction of 21.34% of the unserved loads in the restoration process of power systems. In addition, it was shown that the improve restoration process of power systems has a significant dependence on the initial value of PSH capacity.

The second case was scrutinized in three seperate sub-cases. The first sub-case depicted the destructive impact of ignoring the NGN constraint, which has not been taken into consideration the previous restoration studies. The outcomes show that considering NGN, results in less restored power. Therefore, there is a huge discrepancy between the studies that have ignored the NGN model since 273.74 MWh of loads remained unserviced. The second sub-case studied the mitigating impact of including a gas storage system in the restoration model. The results point out that a natural gas storage system would ameliorate the restoration load of 45.69 MWh. Eventually, the model in the third sub-case was devised to use the NGN pipelines in a linepack model that allows to store extra energy in the NGN. It was noted that through the optimization process the natural gas was stored in the NGN pipelines and released back to the system at critical restoration time steps, thereby leading to 71.92 MWh of extra resorted power.

The focus of the third case study was to illustrate the impact of different uncertainty-handling methods in the restoration process, and use the state-of-the-art DRO approach. The obtained numerical values showed that DRO model strike a veritable balance between the advantages of conventional RO and SP models. It is not as over-conservative as the RO, while it also does not require the exact probability distribution functions and numerous scenarios that are the foundation of the SP approaches.

VII. COMPARISON

Compared to similar studies [8], [7], [9], [10], [12], [13], [17], [19], the obtained results show that modeling the limitations of the NGN is very critical in restoration the power network. The high penetration of GFU in modern power systems has made the restoration of the power grid completely dependent

on the behavior of the NGN. The escalation of congestion within the natural gas pipeline, especially in the winter seasons, leads to new challenges in the operation of power systems in normal and emergency conditions.

The results obtained in works [10], [25], and [40] show that the robust optimization method provides an overly conservative solution and leads to imposing additional costs on network operators. On the other hand, the extracted results of tasks [18] and [33] rely on stochastic optimization. However, we do not always have access to the exact probability distributions for modeling the stochastic optimization method. To cover the above gaps, we have proposed the moment-based DRO approach for modeling the uncertain behavior of wind power units. The moment-based DRO method provides a robust solution that avoids excessive conservatism of wind power units in the power system restoration process.

The results obtained in works [31] and [32] show that the authors have neglected the contribution of renewable energy sources due to their uncertain behavior in restoring power systems. However, neglecting the participation of renewable energy sources leads to an increase in the restoration time of power systems. Accurate modeling of uncertain behavior and preparation of the desired requirements for the participation of renewable energy sources in the power system restoration process leads to the improvement of the resilience of power networks and the acceleration of network recovery.

VIII. CONCLUSION

In this paper, a decentralized ATC optimization approach was presented to investigate the impact of NGN constraints on the TS restoration process, considering the PSH and high penetration of wind farms. The ATC algorithm decentralizes the problem and finds the point equilibrium in an iterative framework. Unlike the centralized optimization models, the proposed decentralized approach ensure the privacy of each operator, while giving them the freedom to minimize their own independent objective. Moreover, the effects of using GSS and linepack technology in improving the restoration of the TS was studied. In this article, the DRO method was used to model the uncertain behavior of wind farms in the restoration process. The proposed approach was investigated in the framework of three case studies, the results of which are summarized as follows:

- The use of wind farms with all its uncertainties can lead to a significant improvement in the restoration process of power grids. In addition, they can reduce the excessive dependence of electricity generation on the NGN. Restoring the bulk power system in the presence of wind energy sources leads to a 16.35% reduction in unserved loads, which is equal to 361.995 MWh of energy. Furthermore, the restoration of the bulk power system, in the coordination of wind farms and PSH, results in a substantial 21.34% reduction in unserved loads. This reduction is equivalent to a remarkable 472.39 MWh of energy.
- Ignoring the constraints of the NGN in the process of restoring the TS can lead to unrealistic and wrong decisions. Because the gas fuel consumption of GFUs depends on the NGN. Therefore, the impact of the pressure limit in the nodes, the maximum transferable natural gas capacity, the behavior of the gas flow in the pipelines, and the possibility of the overlap of the peak times of the electricity and NGNs must be investigated in the process of restoring the TS. Restoring the power grid in the presence of NGN constraint leads to an increase of 11.92% or 273.74 MWh in unserviced loads
- The use of GSSs and linepack technology can improve the restoration process of the TS. The reason is that releasing the energy stored in GSSs and linepack technology, leads to an increase in fuel supply to GFUs. In addition, the use of these technologies leads to an increase in the flexibility of the NGN. Overall, considering the GSS and line pack technology leads to a reduction of 1.98% and 2.09% of unserviced loads, respectively.
- Solving the TS restoration problem in the DRO framework leads to providing a robust solution, which avoids overly conservative solutions such as conventional RO.

As a direction for future studies, it was noted that the presence of active distribution systems has not been investigated together with NGN models. Furthermore, comparison between various decentralized restoration approaches is relatively under-researched area in the topic of power system restoration

ACKNOWLEDGMENT

This work was supported by the Luxembourg National Research Fund (FNR) LightGridSEED Project, ref. C21/IS/16215802 LightGridSEED. For the purpose of open access, and in fulfilment of the obligations arising from the grant agreement, the author has applied a Creative Commons Attribution 4.0 International (CC BY 4.0) license to any Author Accepted Manuscript version arising from this submission.

REFERENCES

[1] M. Farrokhifar, Y. Nie, and D. Pozo, "Energy systems planning: A survey on models for integrated power and natural gas networks coordination," *Appl. Energy*, vol. 262, Mar. 2020, Art. no. 114567.

[2] C. Lv, H. Yu, P. Li, K. Zhao, H. Li, and S. Li, "Coordinated operation and planning of integrated electricity and gas community energy system with enhanced operational resilience," *IEEE Access*, vol. 8, pp. 59257–59277, 2020.

[3] F. Qi, M. Shahidehpour, F. Wen, Z. Li, Y. He, and M. Yan, "Decentralized privacy-preserving operation of multi-area integrated electricity and natural gas systems with renewable energy resources," *IEEE Trans. Sustain. Energy*, vol. 11, no. 3, pp. 1785–1796, Jul. 2020.

[4] M. Sang, Y. Ding, M. Bao, S. Li, C. Ye, and Y. Fang, "Resilience-based restoration strategy optimization for interdependent gas and power networks," *Appl. Energy*, vol. 302, Nov. 2021, Art. no. 117560.

[5] Y. Weng, S. Ly, P. Wang, and H. D. Nguyen, "Hypothesis testing for mitigation of operational infeasibility on distribution system under rising renewable penetration," *IEEE Trans. Sustain. Energy*, vol. 14, no. 2, pp. 876–891, Apr. 2023.

[6] *Black Start from Non-Traditional Generation Technologies: Technology Capability and Readiness for Distributed Restoration*, National Grid ESO, Warwick, U.K., Jun. 2019.

[7] A. Golshani, W. Sun, Q. Zhou, Q. P. Zheng, J. Wang, and F. Qiu, "Coordination of wind farm and pumped-storage hydro for a self-healing power grid," *IEEE Trans. Sustain. Energy*, vol. 9, no. 4, pp. 1910–1920, Oct. 2018.

[8] A. Golshani, W. Sun, Q. Zhou, Q. P. Zheng, and Y. Hou, "Incorporating wind energy in power system restoration planning," *IEEE Trans. Smart Grid*, vol. 10, no. 1, pp. 16–28, Jan. 2019.

[9] J. Zhao, H. Wang, Q. Wu, N. D. Hatziargyriou, and F. Shen, "Distributed risk-limiting load restoration for wind power penetrated bulk system," *IEEE Trans. Power Syst.*, vol. 35, no. 5, pp. 3516–3528, Sep. 2020.

[10] J. Zhao, H. Wang, Y. Hou, Q. Wu, N. D. Hatziargyriou, W. Zhang, and Y. Liu, "Robust distributed coordination of parallel restored subsystems in wind power penetrated transmission system," *IEEE Trans. Power Syst.*, vol. 35, no. 4, pp. 3213–3223, Jul. 2020.

[11] M. Wang, Z. Fan, J. Zhou, and S. Shi, "Research on urban load rapid recovery strategy based on improved weighted power flow entropy," *IEEE Access*, vol. 9, pp. 10634–10644, 2021.

[12] Y. Jiang and T. H. Ortmeyer, "Propagation-based network partitioning strategies for parallel power system restoration with variable renewable generation resources," *IEEE Access*, vol. 9, pp. 144965–144975, 2021.

[13] J. Zhao, Q. Wu, N. D. Hatziargyriou, F. Li, and F. Teng, "Decentralized data-driven load restoration in coupled transmission and distribution system with wind power," *IEEE Trans. Power Syst.*, vol. 36, no. 5, pp. 4435–4444, Sep. 2021.

[14] V. Vita, G. Fotis, C. Pavlatos, and V. Mladenov, "A new restoration strategy in microgrids after a blackout with priority in critical loads," *Sustainability*, vol. 15, no. 3, p. 1974, Jan. 2023.

[15] G. Fotis, V. Vita, and T. I. Maris, "Risks in the European transmission system and a novel restoration strategy for a power system after a major blackout," *Appl. Sci.*, vol. 13, no. 1, p. 83, Dec. 2022.

[16] A. Arab, A. Khodaei, S. K. Khator, and Z. Han, "Electric power grid restoration considering disaster economics," *IEEE Access*, vol. 4, pp. 639–649, 2016.

[17] S. Liu, C. Chen, Y. Jiang, Z. Lin, H. Wang, M. Waseem, and F. Wen, "Bi-level coordinated power system restoration model considering the support of multiple flexible resources," *IEEE Trans. Power Syst.*, vol. 38, no. 2, pp. 1583–1595, Mar. 2023.

[18] A. Kavousi-Fard, M. Wang, and W. Su, "Stochastic resilient post-hurricane power system recovery based on mobile emergency resources and reconfigurable networked microgrids," *IEEE Access*, vol. 6, pp. 72311–72326, 2018.

[19] L. Sun, W. Liu, C. Y. Chung, M. Ding, R. Bi, and L. Wang, "Improving the restorability of bulk power systems with the implementation of a WF-BESS system," *IEEE Trans. Power Syst.*, vol. 34, no. 3, pp. 2366–2377, May 2019.

[20] Y. Lin, B. Chen, J. Wang, and Z. Bie, "A combined repair crew dispatch problem for resilient electric and natural gas system considering reconfiguration and DG islanding," *IEEE Trans. Power Syst.*, vol. 34, no. 4, pp. 2755–2767, Jul. 2019.

[21] M. Yan, Y. He, M. Shahidehpour, X. Ai, Z. Li, and J. Wen, "Coordinated regional-district operation of integrated energy systems for resilience enhancement in natural disasters," *IEEE Trans. Smart Grid*, vol. 10, no. 5, pp. 4881–4892, Sep. 2019.

[22] J. Wei, X. Gao, P. Cheng, W. Fu, and H. Zeng, "Coordinated post-disaster recovery and assessment method for integrated electricity-gas-transportation system," *IEEE Access*, vol. 11, pp. 11685–11699, 2023.

[23] L. Hao, W. Hu, C. Wang, G. Wang, Y. Sun, J. Chen, and X. Pan, "Coordinated restoration optimization of power-gas integrated energy system with mobile emergency sources," *Global Energy Interconnection*, vol. 6, no. 2, pp. 205–227, Apr. 2023.

[24] S. Jafarpour and M. H. Amirioun, "A resilience-motivated restoration scheme for integrated electricity and natural gas distribution systems using adaptable microgrid formation," *IET Gener., Transmiss. Distrib.*, vol. 17, no. 23, pp. 5223–5239, Dec. 2023.

[25] Y. Li, Z. Li, F. Wen, and M. Shahidehpour, "Minimax-regret robust co-optimization for enhancing the resilience of integrated power distribution and natural gas systems," *IEEE Trans. Sustain. Energy*, vol. 11, no. 1, pp. 61–71, Jan. 2020.

[26] F. S. Gazijahani, J. Salehi, and M. Shafie-khah, "Benefiting from energy-hub flexibilities to reinforce distribution system resilience: A pre- and post-disaster management model," *IEEE Syst. J.*, vol. 16, no. 2, pp. 3381–3390, Jun. 2022.

[27] B. Li, Y. Chen, W. Wei, Z. Wang, and S. Mei, "Online coordination of LNG tube trailer dispatch and resilience restoration of integrated power-gas distribution systems," *IEEE Trans. Smart Grid*, vol. 13, no. 3, pp. 1938–1951, May 2022.

[28] A. R. Sayed, C. Wang, and T. Bi, "Resilient operational strategies for power systems considering the interactions with natural gas systems," *Appl. Energy*, vol. 241, pp. 548–566, May 2019.

[29] V. Shabazbegian, H. Ameli, M. T. Ameli, G. Strbac, and M. Qadrdan, "Co-optimization of resilient gas and electricity networks; a novel possibilistic chance-constrained programming approach," *Appl. Energy*, vol. 284, Feb. 2021, Art. no. 116284.

[30] S. Huang, Q. Wu, J. Zhao, and W. Liao, "Distributed optimal voltage control for VSC-HVDC connected large-scale wind farm cluster based on analytical target cascading method," *IEEE Trans. Sustain. Energy*, vol. 11, no. 4, pp. 2152–2161, Oct. 2020.

[31] Z. Z. Lin and F. S. Wen, "Discussion on 'optimal generator start-up strategy for bulk power system restoration,"' *IEEE Trans. Power Syst.*, vol. 27, no. 3, p. 1712, Aug. 2012.

[32] A. Golshani, W. Sun, Q. Zhou, Q. P. Zheng, and J. Tong, "Two-stage adaptive restoration decision support system for a self-healing power grid," *IEEE Trans. Ind. Informat.*, vol. 13, no. 6, pp. 2802–2812, Dec. 2017.

[33] C. Ordoudis, P. Pinson, and J. M. Morales, "An integrated market for electricity and natural gas systems with stochastic power producers," *Eur. J. Oper. Res.*, vol. 272, no. 2, pp. 642–654, Jan. 2019.

[34] M. Z. Oskouei, H. Mehrjerdi, D. Babazadeh, P. T. Baboli, C. Becker, and P. Palensky, "Resilience-oriented operation of power systems: Hierarchical partitioning-based approach," *Appl. Energy*, vol. 312, Apr. 2022, Art. no. 118721.

[35] N. Nasiri, S. Zeynali, S. N. Ravadanegh, S. Kubler, and Y. Le Traon, "A convex multi-objective distributionally robust optimization for embedded electricity and natural gas distribution networks under smart electric vehicle fleets," *J. Cleaner Prod.*, vol. 434, Jan. 2024, Art. no. 139843.

[36] Z. Liu, L. Wang, and L. Ma, "A transactive energy framework for coordinated energy management of networked microgrids with distributionally robust optimization," *IEEE Trans. Power Syst.*, vol. 35, no. 1, pp. 395–404, Jan. 2020.

[37] C. Shang and F. You, "Distributionally robust optimization for planning and scheduling under uncertainty," *Comput. Chem. Eng.*, vol. 110, pp. 53–68, Feb. 2018.

[38] D. Bertsimas and M. Sim, "Robust discrete optimization and network flows," *Math. Program.*, vol. 98, nos. 1–3, pp. 49–71, May 2003.

[39] (2023). *Data Repository*. [Online]. Available: https://uniluxembourg-my.sharepoint.com/:x:/g/personal/saeid_zeinali_uni_lu/EYlzlU7Le61GqUerB5Y-USkBLCDdWRalNs7kfxEMOg3ujw?e=Va4hrI

[40] N. L. Dehghani and A. Shafieezadeh, "Multi-stage resilience management of smart power distribution systems: A stochastic robust optimization model," *IEEE Trans. Smart Grid*, vol. 13, no. 5, pp. 3452–3467, Sep. 2022.

N. NASIRI (Student Member, IEEE) received the B.S. degree in electrical engineering from the Technical University of Tabriz, Tabriz, Iran, in 2017, and the M.S. degree in electrical engineering from the University of Sahand, Tabriz, in 2020. He is currently pursuing the Ph.D. degree in electrical engineering with Azarbaijan Shahid Madani University, Tabriz. His research interests include multi-energy systems, integrated energy markets, peer-to-peer energy transactions, and power system restoration.

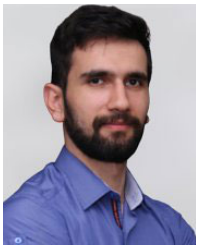

S. ZEYNALI (Student Member, IEEE) is currently pursuing the Ph.D. degree with the Interdisciplinary Centre for Security, Reliability and Trust (SnT), University of Luxembourg. His research interests include applications of distributed and convex optimization methods in power systems, traffic networks, and transportation electrification.

S. NAJAFI RAVADANEGH (Senior Member, IEEE) received the Ph.D. degree in electrical engineering from the Department of Electrical Engineering, Amirkabir University of Technology (Tehran Polytechnic), Tehran, Iran, in 2009. He is currently a Professor with the Electrical Engineering Department, Azarbaijan Shahid Madani University, Tabriz, Iran, where he is responsible for the Resilient Smart Grids Research Laboratory.

S. KUBLER (Senior Member, IEEE) is currently a Research Scientist with the Interdisciplinary Centre for Security, Reliability and Trust (SnT), University of Luxembourg. He had a leading role in several EU projects. He has broad expertise in decision support systems using artificial intelligence (AI), with a focus on how to ensure their trustworthiness, which is a key requirement of the AI Act and the Ethics Guidelines for Trustworthy AI published by the European Commission. He received the Best Thesis Award in Automatic Control from the IFAC French Workgroup GdR MACS/Club EEA.

Y. LE TRAON (Fellow, IEEE) is currently a Full Professor of computer science with the University of Luxembourg, in the domain of software engineering, with a focus on software testing, software security, and data-intensive systems. He is also the Director of the Interdisciplinary Centre for Security, Reliability and Trust (SnT).